PNAS RESEARCH ARTICLE | PHARMACOLOGY OPEN ACCESS

Structure-based design of selective, orally available salt-inducible kinase inhibitors that stimulate bone formation in mice

Tadatoshi Sato[a,b,c], Christian D. Castro Andrade[a], Sung-Hee Yoon[a], Yingshe Zhao[a], William J. Greenlee[d], Patricia C. Weber[d], Usha Viswanathan[e], John Kulp[e], Daniel J. Brooks[a], Marie B. Demay[a], Mary L. Bouxsein[a], Bruce Mitlak[f], Beate Lanske[f], and Marc N. Wein[a,g,h,1]

Edited by Gerald Shulman, Yale University, New Haven, CT; received August 22, 2022; accepted November 11, 2022

Osteoporosis is a major public health problem. Currently, there are no orally available therapies that increase bone formation. Intermittent parathyroid hormone (PTH) stimulates bone formation through a signal transduction pathway that involves inhibition of salt-inducible kinase isoforms 2 and 3 (SIK2 and SIK3). Here, we further validate SIK2/SIK3 as osteoporosis drug targets by demonstrating that ubiquitous deletion of these genes in adult mice increases bone formation without extraskeletal toxicities. Previous efforts to target these kinases to stimulate bone formation have been limited by lack of pharmacologically acceptable, specific, orally available SIK2/SIK3 inhibitors. Here, we used structure-based drug design followed by iterative medicinal chemistry to identify SK-124 as a lead compound that potently inhibits SIK2 and SIK3. SK-124 inhibits SIK2 and SIK3 with single-digit nanomolar potency in vitro and in cell-based target engagement assays and shows acceptable kinome selectivity and oral bioavailability. SK-124 reduces SIK2/SIK3 substrate phosphorylation levels in human and mouse cultured bone cells and regulates gene expression patterns in a PTH-like manner. Once-daily oral SK-124 treatment for 3 wk in mice led to PTH-like effects on mineral metabolism including increased blood levels of calcium and 1,25-vitamin D and suppressed endogenous PTH levels. Furthermore, SK-124 treatment increased bone formation by osteoblasts and boosted trabecular bone mass without evidence of short-term toxicity. Taken together, these findings demonstrate PTH-like effects in bone and mineral metabolism upon in vivo treatment with orally available SIK2/SIK3 inhibitor SK-124.

kinase inhibitor | parathyroid hormone | osteoporosis

Significance

Orally available therapies are desperately needed to stimulate bone formation for patients with osteoporosis. Parathyroid hormone can increase bone formation, and a key step in the intracellular action of PTH downstream of protein kinase A is to inhibit salt-inducible kinase isoforms 2 and 3. Here, we established the safety of targeting SIK2 and SIK3 using genetically modified mice and then used structure-based drug design followed by iterative medicinal chemistry to identify selective, orally available SIK2/SIK3 inhibitors. A lead compound, SK-124, increases bone formation and bone mass when given to mice by once-daily oral treatment. These findings support the further development of specific SIK2/SIK3 inhibitors as a class of bone anabolic osteoporosis therapies.

Osteoporosis affects over 20 million Americans leading to 1.5 million fragility fractures every year (1, 2). The most frequently used osteoporosis medications act by inhibiting osteoclastic bone resorption. These antiresorptive drugs only increase bone mineral density (BMD) and reduce hip fractures modestly (3). Due to side effects associated with long-term use, guidelines suggest that antiresorptive therapies should be used for only 3 to 5 consecutive years (4, 5). Analogs of parathyroid hormone (PTH) are the most commonly used bone anabolic agents (6). While effective, PTH-based agents are limited by the need for daily injections, a major barrier for patients with a chronic, asymptomatic disease (7). Use of the antisclerostin antibody romosozumab is limited by the need for monthly high-volume injections, waning anabolic efficacy over time, and risk of cardiovascular events in at-risk patients (8). Therefore, safe, orally available bone anabolic agents represent a critical unmet need for this major public health problem.

Recent advances in PTH1R structural biology have suggested new ways to modify PTH1R peptide agonists to optimize bone formation (9–12). However, small-molecule PTH receptor agonists show poor binding affinity (13), and peptide modification to promote oral bioavailability (14) leads to unpredictable pharmacokinetics and suboptimal efficacy (15). Therefore, knowledge regarding downstream steps in PTH action is needed to inform future pharmacologic efforts to target this pathway with drug-like orally available compounds.

Salt-inducible kinases (SIKs) are AMPK-family serine/threonine kinases. Although SIK1 is induced by dietary salt intake in the adrenal gland (16), SIK2 and SIK3 are broadly expressed and are not regulated by dietary salt. Rather, SIK2/SIK3 activity is induced by kinase domain phosphorylation by LKB1 and inhibited by cAMP/protein kinase A (PKA)–dependent phosphorylation, which blocks cellular SIK activity via an allosteric mechanism (17). We demonstrated a central role of SIKs in PTH action: In the absence of PTH/cAMP signaling, SIK activity in cells is constitutively "on," leading to phosphorylation and cytosolic retention of SIK substrates such as class IIa HDAC proteins and CRTC coactivators (18). PTH signaling leads to PKA-dependent SIK phosphorylation, which in turn inhibits SIK cellular activity (19). Small-molecule SIK inhibitors, such as YKL-05-099 (20, 21), a

Competing interest statement: The authors declare competing interest. B.M. and B.L. are employees of Radius Health. M.N.W. holds equity in and is a scientific advisory board member of Relation Therapeutics. M.N.W. is a co-inventor on pending patents regarding the use and composition of SIK inhibitors for osteoporosis. W.J.G. is a co-inventor on a pending patent regarding the composition of SIK inhibitors for osteoporosis. M.N.W. receives research funding from Radius Health.

This article is a PNAS Direct Submission.

[1]To whom correspondence may be addressed. Email: mnwein@mgh.harvard.edu.

This article contains supporting information online at https://www.pnas.org/lookup/suppl/doi:10.1073/pnas.2214396119/-/DCSupplemental.

Published December 6, 2022.

nonselective compound that inhibits all three SIK isoforms, mimic skeletal actions of PTH in vitro and in vivo (22, 23). Human and mouse genetics reveal a key role of SIK2/SIK3 downstream of PTH1R action in bone growth and remodeling (24, 25). In contrast, SIK1 plays a key role in blood pressure and renal salt handling (26); as such, selective SIK2/SIK3 inhibitors are desired to increase bone formation without cardiovascular toxicities.

In this study, we defined the organismal consequences of ubiquitous SIK2/SIK3 deletion in skeletally mature animals. Motivated by observing increased bone formation without overt extraskeletal toxicities, we proceeded to use structure-based drug design to identify and develop compounds that selectively target these SIK isoforms. From these efforts, we identify SK-124 as a lead compound with potent SIK2/SIK3 inhibitory activity in vitro and in cells. Furthermore, oral administration of this compound showed PTH-like effects at the level of mineral metabolism and, most importantly, stimulated bone formation and increased bone mass.

Results

Inducible, ubiquitous SIK2/SIK3 gene deletion provides a powerful in vivo mouse model to interrogate skeletal and extraskeletal effects of targeting these kinases. In previous work, we focused on short-term (~3 wk) studies in young/growing mice (23). Since osteoporosis is a chronic disease, it is crucial to define the long-term safety profile. Therefore, we treated 12-wk-old control (*Sik2*$^{f/f}$; *Sik3*$^{f/f}$) and mutant (*Sik2*$^{f/f}$; *Sik3*$^{f/f}$; ubiquitin-Cre^{ERt2}) mice with tamoxifen and then assessed phenotypes 2, 4, 8, and 16 wk later. Serum analysis showed dramatic increases in bone turnover markers alkaline phosphatase, N terminal propeptide of type I collagen (P1NP), and CTX following inducible SIK2/SIK3 deletion (Fig. 1*A*). Histology analysis of tibia sections revealed expansion of trabecular bone, increased marrow stromal cells, and growth plate expansion in compound mutant mice (Fig. 1 *B* and *C*). Growth plate expansion is likely due to SIK3-mediated control of chondrocyte hypertrophy downstream of PTHrP (25, 27), a phenotype of low relevance to adult humans whose growth plate is resorbed by estrogen-dependent mechanisms at the time of puberty (28). Consistent with our previous reports (23, 25), inducible SIK2/SIK3 deletion reduced sclerostin immunoreactivity in osteocytes (Fig. 1*D*). Micro-CT demonstrated progressive filling of the bone marrow cavity with trabecular bone and increased cortical bone mass upon global SIK2/SIK3 deletion (Fig. 1*E* and Dataset S1). Importantly, these dramatic skeletal phenotypes occurred without changes in other serum chemistries or blood counts (*SI Appendix*, Fig. S1 *A* and *B*). Together, these findings justified efforts to develop specific SIK2/SIK3 inhibitors to stimulate bone formation.

At the outset of our program, there were no reports of selective SIK2/SIK3 inhibitors, and no SIK X-ray crystal structure had been reported. A SIK2 homology model (Fig. 2*A*) was created based on microtubule affinity–regulating kinase 3 (MARK3; PDB entry 2QNJ, 55% kinase domain sequence identity), and a virtual screen of 100,000 compounds was performed to identify compounds with predicted binding to the SIK2 active site. Since previous SIK inhibitors such as YKL-05-099 are nonselective (23), we filtered in silico "hits" against p38α and SRC (two kinases also targeted by YKL-05-099). Further selection of in silico hits was performed by a comparison with three known potent SIK2 inhibitors (YKL-05-099, AZD-7762 (29), and crenolanib) with Ligand Similarity using Clique Algorithm (30).

The most potent initial hit structure 1 (Fig. 2*B*) was chosen as a starting point for optimization. A total of 60 commercially available analogs of 1 were screened, and from this, set inhibitor 2 (Fig. 2*B*) was identified as a submicromolar SIK2 inhibitor using a radioisotope kinase assay with full-length SIK2 and AMARAASAAALARRR peptide substrate. Modifications of inhibitor 2 focused on replacements for the benzimidazole scaffold allowed the imidazopyridine inhibitor 6 to be identified as a potent SIK2 inhibitor with substantial SIK3 inhibitory activity (Fig. 2*C*). In contrast, isomeric imidazopyridine 3, pyrazolopyridine 4, and benzotriazole 5 were less potent. We expected that the methoxy substituents of 6 would be potential sites of metabolism and therefore explored replacements (Fig. 2*D*). The best of these was 4-cyano in inhibitor 10, which gave comparable SIK2 potency, although reduced SIK3 potency. Addition of a second substituent to the phenyl ring of 10 (inhibitors 11 and 12) led to loss of potency. Replacement of the pyridine ring in the 3-pyridylmethyl amide of inhibitor 10 with other heterocycles (4-pyridazinyl, 2-pyrazinyl, 2-furanyl, 2-benzoxazol-yl, and benzimidazol-2-yl) gave inhibitors with equivalent or reduced potency at SIK2.

Although imidazopyridine 10 was found to have good stability in rat and human microsomes (Dataset S2), we were concerned about stability of the amide bond in vivo. Thus, we explored replacement of the amide-containing substituent with an ether or a heterocycle. Of many amide replacements synthesized (Fig. 2*E*), ether inhibitor 13 and pyrazole inhibitor 14 emerged as particularly promising. Similar to the development of a related series of SIK inhibitors (31, 32), we decided to incorporate two methoxy substituents into the modestly potent 1,3,4-oxadiazole analog 15 (which was synthesized from the 4-cyano inhibitor 14), which resulted in the potent inhibitor 16 (SK-124), which was nearly equipotent at SIK2 and SIK3, and had 15-fold selectivity versus SIK1. A similar level of potency was observed for the related inhibitors 17 and 18 and for the 1,2,4-oxadiazole analog 19 (*SI Appendix*, Fig. S2), while the monomethoxy analog 20 showed slightly reduced potency. Interestingly, replacement of the methoxy groups with fluoro, chloro, or methyl substituents reduced inhibitor SIK2 potency. Of note, compounds generated here are structurally distinct from those recently reported to inhibit SIK2 and PAK (33, 34). Compound 16 has drug-like features with respect to drug metabolism and pharmacokinetics (Dataset S2). This compound displays acceptable oral bioavailability in mice (*SI Appendix*, Fig. S3), robust stability in human, rat, and mouse liver microsomes, no inhibition of cytochrome P450 enzymes, and no significant off-target activities at 10 μM (Dataset S3) in the Eurofins SafetyScreen44 panel (35).

Achieving specificity is a particular challenge in development of ATP-competitive kinase inhibitors for SIKs due to the presence of a gatekeeper threonine residue (36, 37). As expected (20, 23, 34), activity-based profiling of YKL-05-099 at 0.5 μM in a panel of 300 kinases using a microfluidic-based system (Nanosyn (38)) demonstrated that this compound targets multiple tyrosine kinases, with 43/300 kinases inhibited >80% at this dose (Fig. 3*A*). In contrast, 16 (hereafter referred to as SK-124) (0.5 μM) showed considerably improved specificity in this panel, with inhibition of 9/300 kinases tested (two of which include SIK isoforms) (Fig. 3 *A* and *B*; Dataset S4 shows Nanosyn results for compounds 13, 14, 16, 17, 18, 20, and YKL-05-099). Further assessment of all "off-target" kinases inhibited by 16 in single-dose kinome profiling using 10-point IC_{50} assays demonstrated specificity of this compound for SIK2, with PDGFRα (IC_{50} 15.8 nM) as the major off-target kinase inhibited (Dataset S4).

Based on these in vitro results, we assessed cell-based target engagement for this lead series. First, NanoBRET assays in HEK293T cells expressing SIK–NanoLuc constructs (39) confirmed SIK target engagement, with cell-based IC_{50} values for SIK2 and SIK3 close to values obtained using in vitro kinase assays (Fig. 3*C*). Of note, this assay suggested improved specificity of SK-124 for SIK2/SIK3 versus SIK1 compared with studies using

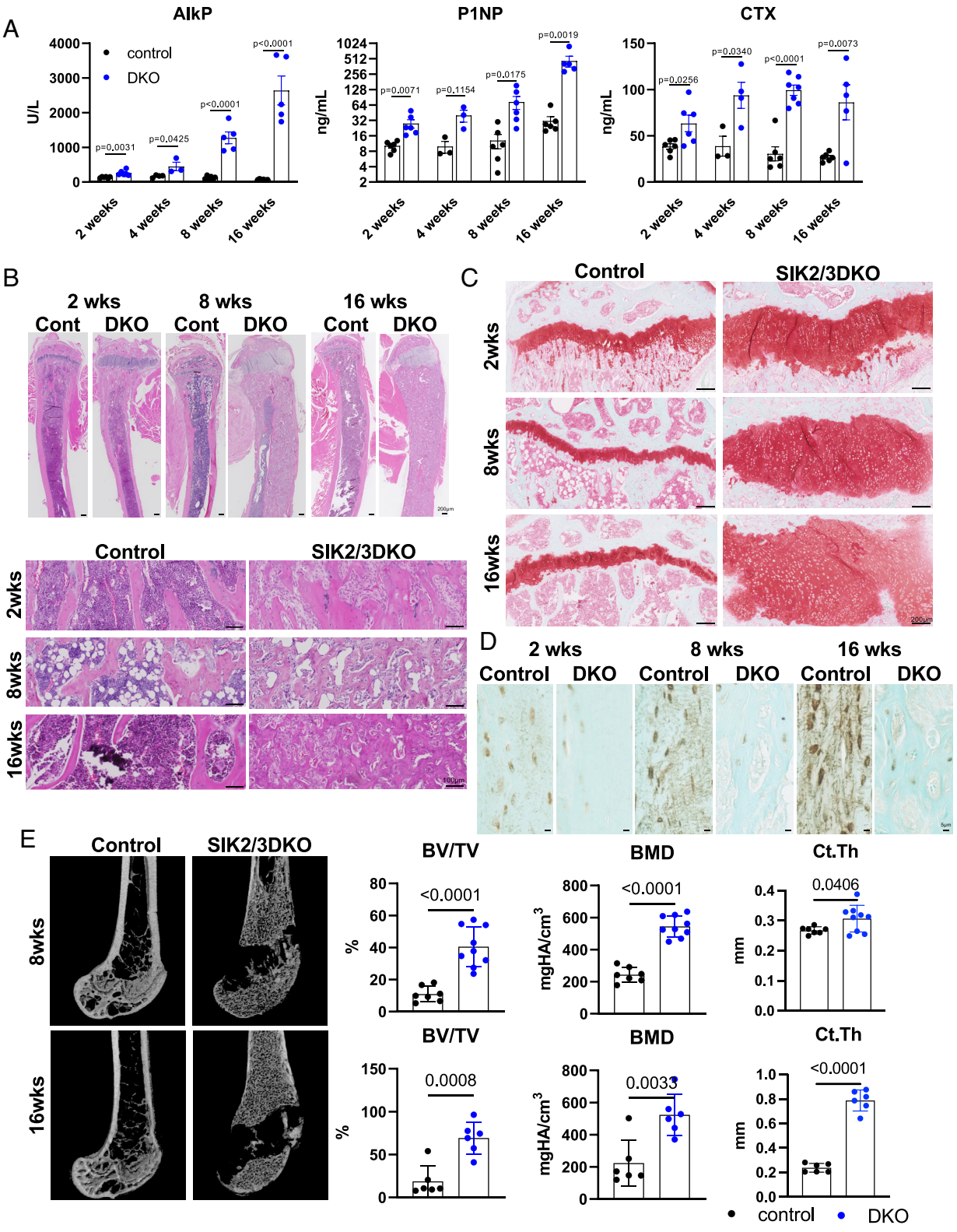

Fig. 1. Whole-body *Sik2/Sik3* ablation increases bone turnover markers and trabecular bone mass. Twelve-week-old control (*Sik2*$^{f/f}$; *Sik3*$^{f/f}$) and mutant (*Sik2*$^{f/f}$; *Sik3*$^{f/f}$; ubiquitin-Cre^{ERt2}) were treated with tamoxifen (1 mg IP Q48H ×3 doses). (*A*) Bone turnover markers (alkaline phosphatase (AlkP), P1NP, and CTX) were measured 2, 4, 8, and 16 wk after tamoxifen treatment. Serum analysis of mice after tamoxifen administration showed dramatic increases in turnover markers at each time point (n = 3 to 6 mice per group). (*B*) Tibia histology by hematoxylin and eosin (HE) stain. (*C*) Safranin O and (*D*) sclerostin immunohistochemistry were performed. Sclerostin levels were substantially down-regulated by *Sik2*/*Sik3* gene deletion at each time point. (*E*) Distal femur micro-CT results showed significantly increased bone volume and mineral density 8 and 16 wk after tamoxifen treatment. Images are shown on the *Left*, and key trabecular (bone volume per tissue volume (BV/TV) and trabecular BMD) and cortical (cortical thickness) parameters are shown on the *Right* (n = 6 to 9 mice per group). See also Dataset S1 for full micro-CT data from 8- and 16-wk chase animals. *P* values versus control are shown in the figure. Two-sided *t* tests were used (*A* and *E*). Data are expressed as mean ± SEM.

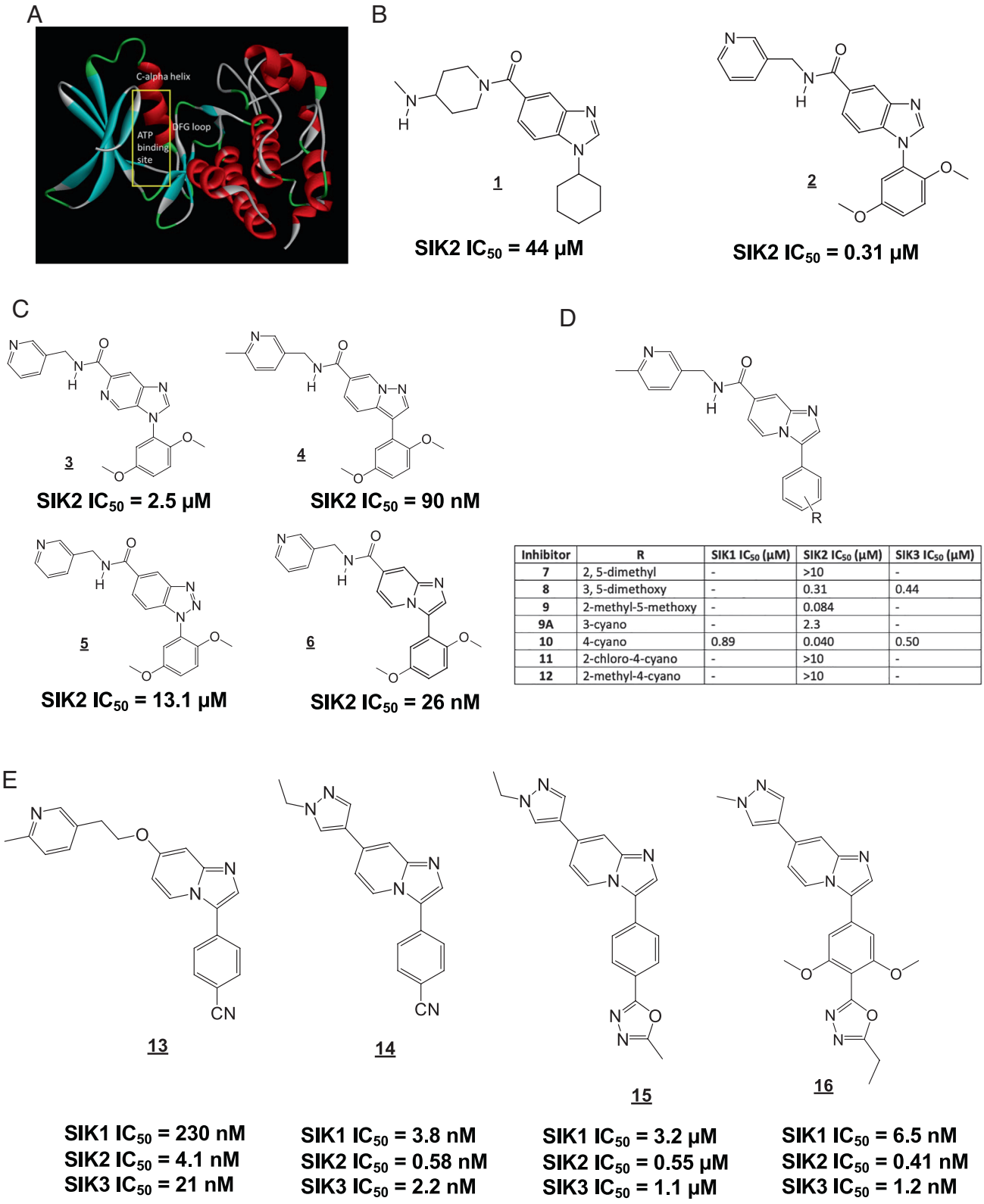

Inhibitor	R	SIK1 IC_{50} (μM)	SIK2 IC_{50} (μM)	SIK3 IC_{50} (μM)
7	2, 5-dimethyl	-	>10	-
8	3, 5-dimethoxy	-	0.31	0.44
9	2-methyl-5-methoxy	-	0.084	-
9A	3-cyano	-	2.3	-
10	4-cyano	0.89	0.040	0.50
11	2-chloro-4-cyano	-	>10	-
12	2-methyl-4-cyano	-	>10	-

Fig. 2. Identification of SK-124 (compound 16) by in silico screening followed by iterative medicinal chemistry. (*A*) Homology model of SIK2 used for in silico docking. (*B–E*) Chemical structures of compounds. SIK2 kinase assay was assessed with a radioisotope kinase assay using recombinant full-length SIK2 and HDAC5 peptide substrate in a 10-point dose–response format. Respective IC_{50} values are indicated below each compound.

recombinant kinases. Next, cell-based thermal shift assays (40) in murine Ocy454 cells demonstrated that SK-124 engages endogenous SIK2 in murine osteocyte-like Ocy454 cells (Fig. 3*D*). Furthermore, treatment of cells with SK-124, but not its inactive analog 15 (SK-128), reduced phosphorylation of SIK substrates HDAC4/HDAC5 and CRTC2 in murine Ocy454 and human Saos2 cells (Fig. 3*E* and *SI Appendix*, Fig. S4*A*), promoted CRTC2 and HDAC5 nuclear translocation (Fig. 3*F* and *SI Appendix*, Fig. S4*B*), and regulated SIK target gene [*SOST* and *TNFSF11* (also known as RANKL)] expression in a PTH-like manner (Fig. 3*G*

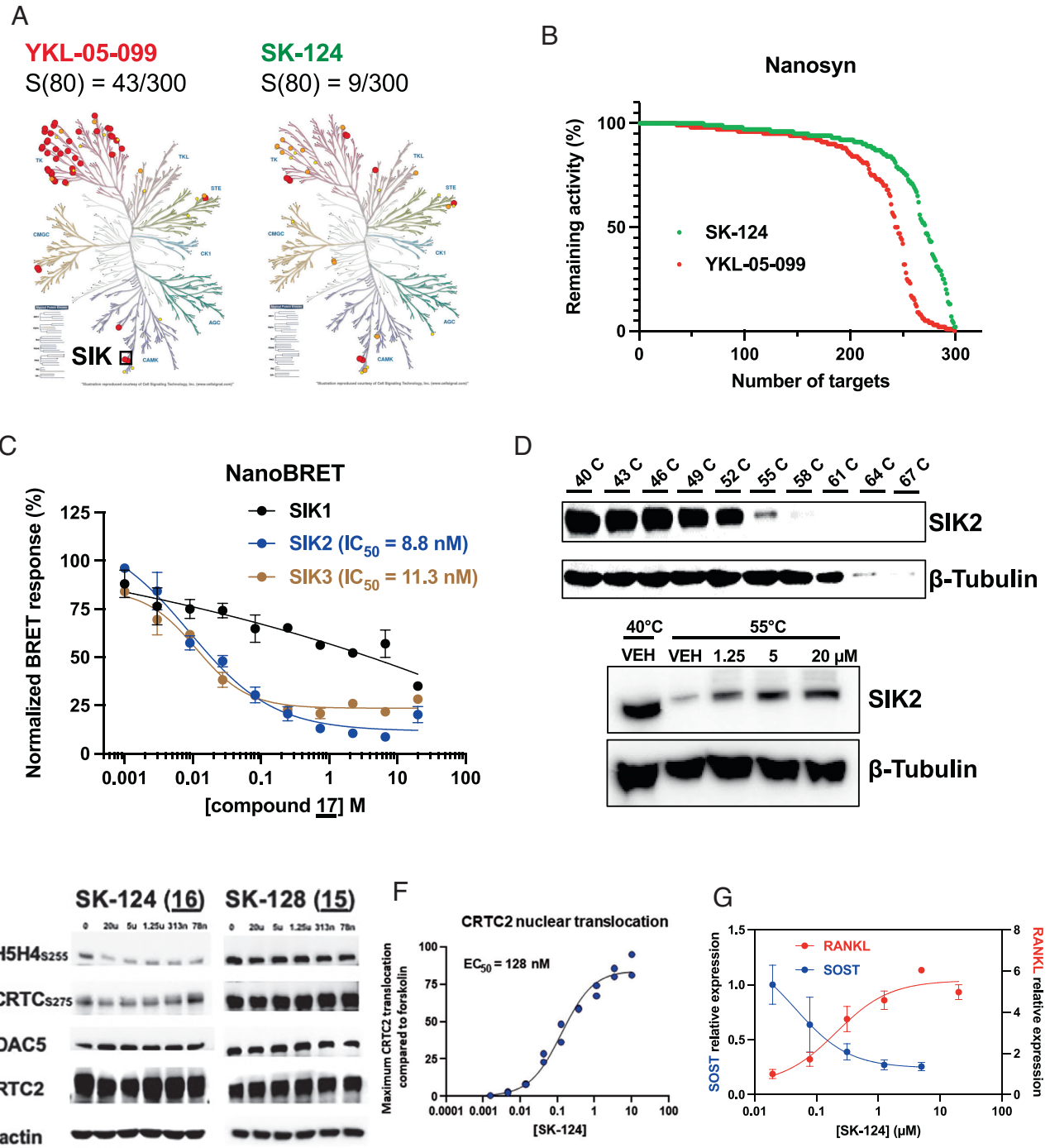

Fig. 3. Kinome selectivity and cellular activity of SK-124. (*A*) YKL-05-099 and SK-124 were tested at 0.5 μM on a panel of 300 human kinases. Dendrograms show kinases inhibited >80% by each compound in red. SIK isoforms are present at the 6-o'clock position. S(80) refers to the portion of kinases tested whose activity was inhibited >80% by 0.5 μM compounds. (*B*) Comparison of SK-124 and YKL-05-099 against 300 kinases as percentage of remaining activity. (*C*) NanoBRET assays using NanoLuc–SIK fusion proteins were performed in HEK293T cells using the indicated doses of SK-124 used for cell-based calculation of IC_{50} values. (*D*) Cellular thermal shift assay was performed in Ocy454 cells. *Top* panels show the melting curve used to determine SIK2 thermostability. A melting temperature of 55 °C was selected for subsequent studies. *Bottom* panels show effects of SK-124 treatment (1 h) on SIK2 thermostability at 55 °C. (*E*) Ocy454 cells were treated with the indicated compounds/doses for 1 h followed by immunoblotting as indicated. (*F*) PathHunter® U2OS CRTC2 (TORC2) nuclear translocation reporter cells were treated for 90 min with the indicated doses of SK-124. Data are reported as CRTC2 nuclear translocation relative to forskolin (10 μM, positive control). (*G*) Ocy454 cells were treated for 4 h with the indicated doses of SK-124 followed by RNA isolation for RT-qPCR, with β-actin used as a housekeeping gene.

and *SI Appendix*, Fig. S4*C*) without causing cytotoxicity (*SI Appendix*, Fig. S4*D*).

Based on its potency, selectivity, drug-like features, and robust activity in bone-relevant cell culture models, we treated 8-wk-old male C57BL/6J mice with SK-124 by once-daily oral gavage (n = 10 mice/group, doses of 2.5 mg/kg/d, 10 mg/kg/d, and 40 mg/kg/d) for a total of 3 wk, a time sufficient to observe changes in trabecular bone in response to YKL-05-099 (22). In addition, we also treated one group of mice with oral vehicle solution (negative control) and another group of mice with once-daily subcutaneous hPTH(1–34) (80 μg/kg) injections (positive control). Mice tolerated SK-124 treatment well without obvious health concerns and weight loss (*SI Appendix*, Fig. S5*A*). Serum was collected 2 h after oral gavage on treatment day 13, and SK-124 serum levels increased in

a dose-dependent manner in the 3 treatment groups (Fig. 4*A*). Serum mineral metabolism parameters were measured in mice in all 5 treatment groups after 21 d of treatment (serum was collected 2 h after the final treatment dose). SK-124 treatment led to PTH–like effects including increased serum calcium (Fig. 4*B*), increased serum 1,25-vitamin D levels, and reduced serum PTH levels. Likely in response to increased serum 1,25-vitamin D levels, high-dose SK-124 treatment increased serum FGF-23 levels. In contrast, SK-124 treatment did not alter serum levels of phosphorus or BUN (Fig. 4*B* and *SI Appendix*, Fig. S5*B*). Taken together, these

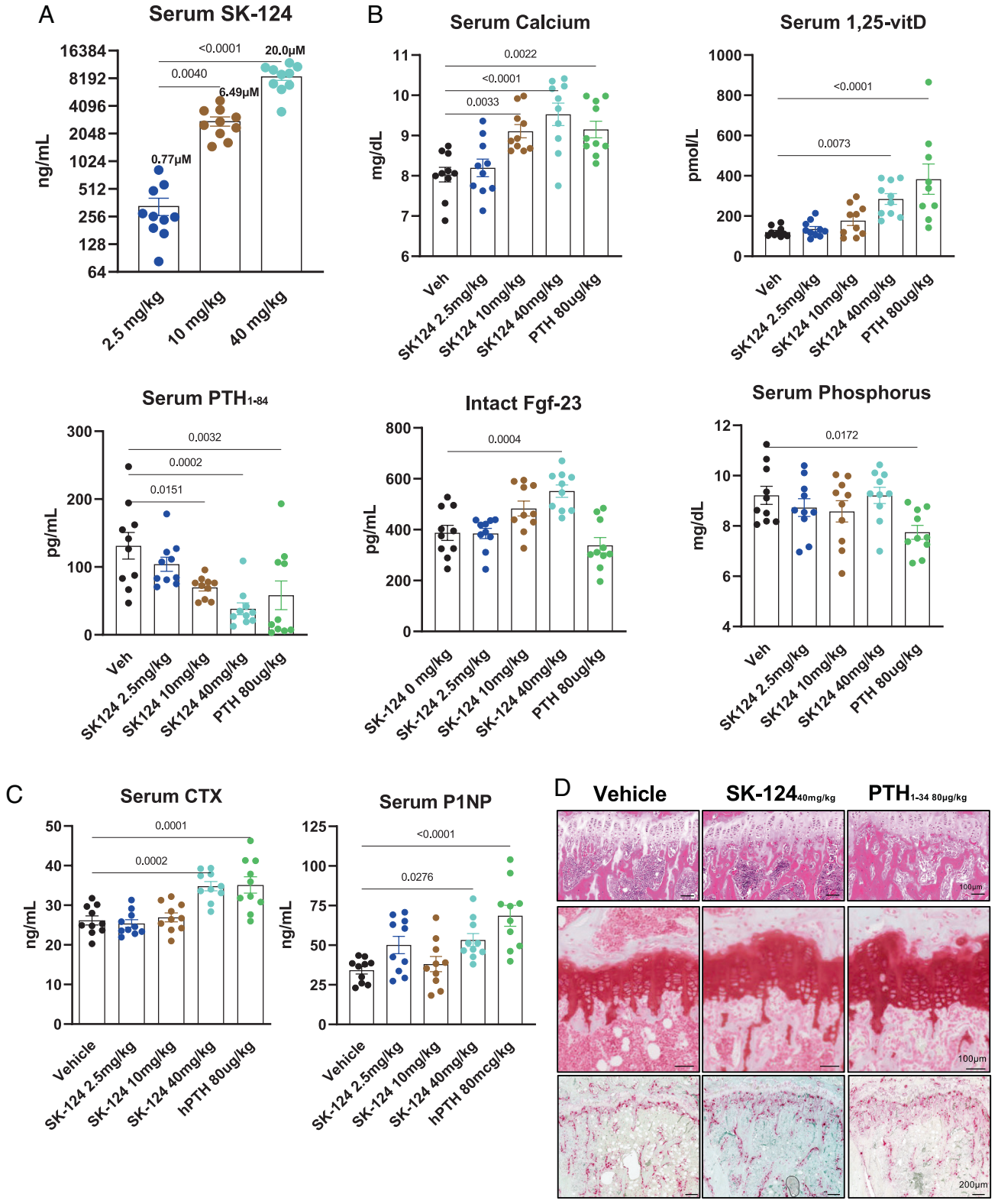

Fig. 4. SK-124 affects mineral metabolism in a PTH-like manner. (*A*) Mice were treated once daily with the indicated doses of SK-124 by oral gavage (n = 10/group). Two hours after dose #14 was administered, serum was collected to measure SK-124 levels by mass spectrometry. (*B* and *C*) 2 h after SK-124 dose #21 was administered, serum was collected to measure the indicated analyte. In all panels, data points represent individual mice. (*D*) Decalcified paraffin-embedded sections from the tibiae of mice after 3 wk of the indicated treatment were stained using hematoxylin and eosin (*Top*), safranin O (*Middle*), and TRAP (*Bottom*).

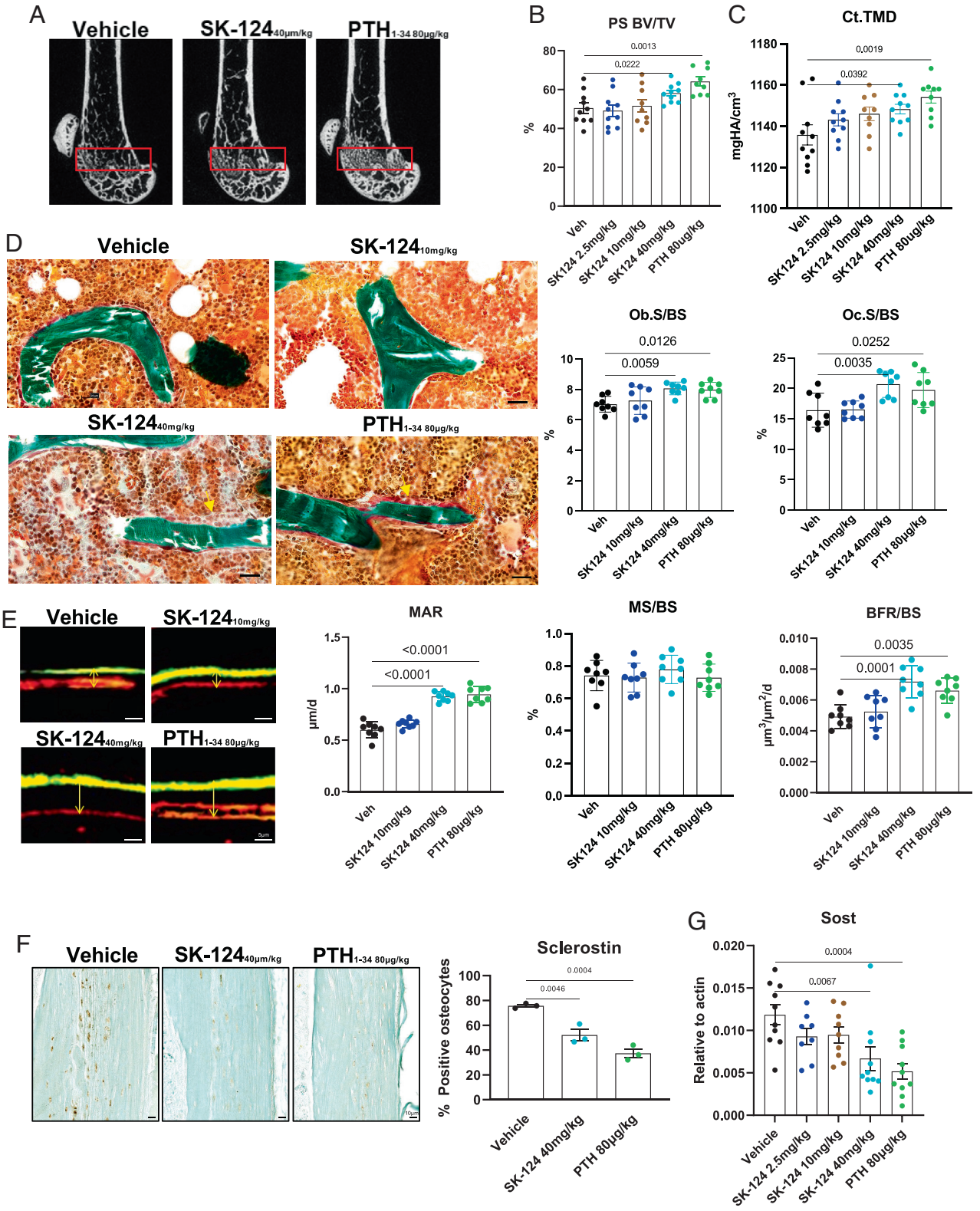

Fig. 5. SK-124 affects bone remodeling in a PTH-like manner. (*A*) Representative micro-CT images from the femur of mice in the indicated treatment group. The red box denotes the PS region. Quantification of (*B*) PS bone volume fracture and (*C*) midshaft cortical TMD in the indicated treatment groups by micro-CT. See also Dataset S5 for complete micro-CT results at all sites analyzed. (*D*) Trichrome-stained sections from histomorphometry study demonstrating increased osteoblasts on trabecular bone surfaces of mice treated with high-dose SK-124 and PTH. Yellow arrowheads denote groups of active osteoblasts seen in response to high-dose SK-124 and PTH. (Scale bar, 20 µm.) Quantification of osteoblast (Ob.S/BS) and osteoclast (Oc.S/BS) measurements is shown on the *Right*. (*E*) Dual calcein (green) and demeclocycline (red) images are shown from mice in the indicated treatment groups. Both high-dose SK-124 and PTH increase MAR and BFR/BS but not the MS/BS. See also Dataset S6 for complete histomorphometry results. (*F*) Sclerostin immunohistochemistry (brown staining) was performed and quantified (*Right*). (*G*) Cortical bone RNA was isolated, and SOST (gene that encodes sclerostin) levels were determined by RT-qPCR. For all panels, one-way ANOVA was performed followed by Tukey's post hoc analysis to compare treatment groups with vehicle. *P* values less than 0.05 are shown on the graphs.

mineral metabolism changes demonstrate a PTH-like effect of SK-124 treatment and support further investigation into the skeletal effects of this compound. Serum bone turnover markers (P1NP, a marker of bone formation; C terminal telopeptide (CTX), a marker of bone resorption) were also measured on samples collected after 21 d of treatment. Oral SK-124 (40 mg/kg) treatment increased P1NP and CTX compared with oral vehicle solution in a manner similar to that of once-daily subcutaneous PTH treatment (Fig. 4*C*). At the histological level, 3 wk of 40 mg/kg SK-124 treatment led to changes consistent with intermittent PTH therapy and inducible SIK2/SIK3 deletion including increased trabecular bone in the primary spongiosa (PS), modest growth plate expansion, and increased TRAP-positive osteoclasts in the proximal tibia (Fig. 4*D*).

Since the initial skeletal response to short-term SK-124 was most dramatic in the PS, we focused subsequent micro-CT analysis on this bone region in the femur. SK-124 (40 mg/kg) treatment increased both PS bone volume fraction (PS BV/TV) and middiaphyseal cortical bone tissue mineral density (TMD) (Fig. 5 *A* and *C* and Dataset S5). Prompted by effects of SK-124 on bone mass, we performed static and dynamic histomorphometry to quantify the effects of this compound at the level of bone cell composition and activity. Similar to once-daily PTH injections, SK-124 (40 mg/kg) treatment increased osteoblast and osteoclast numbers on trabecular bone surfaces (Fig. 5*D*) and increased matrix apposition rate (MAR) and bone formation rate (BFR/BS) without exerting effects on mineralizing surface (MS/BS) (Fig. 5*E* and Dataset S6).

Finally, we explored molecular correlates to explain the changes in bone mass and cellular activity seen in response to SK-124. Consistent with our histology, histomorphometry, and serum data, SK-124 treatment increased expression of the osteoblast marker gene *Spp1* (osteopontin), the osteoclast marker genes *Ctsk* and *Acp5* (cathepsin K and TRAP5b), and Fgf-23 mRNA levels in cortical bone (*SI Appendix*, Fig. S5*C*). Increased osteoclast activity, evident based on increased serum CTX, increased osteoclast numbers, and increased osteoclast gene expression, seen in response to SK-124 treatment is likely due to the ability of this compound to directly stimulate *TNFSF11* receptor activator of NF-kappaB ligand (RANKL) in mesenchymal lineage cells (Fig. 3*G*); unlike YKL-05-099 (which directly blocks osteoclast maturation via off-target actions on M-CSF signaling (23)), in vitro SK-124 treatment did not inhibit osteoclastogenesis (*SI Appendix*, Fig. S6). Similar to our previous studies with nonspecific pan-SIK inhibitors and with SIK2/SIK3 gene deletion, SK-124 treatment reduced sclerostin (an osteocyte-derived inhibitor of bone formation (41)) protein levels (Fig. 5*F*) and gene expression (Fig. 5*G*) in vivo.

Discussion

Here, we describe the identification, synthesis, and in vitro and in vivo skeletal characterization of SK-124, an orally available SIK2/SIK3 inhibitor. Short-term treatment of mice with this compound causes PTH-like effects at the levels of bone remodeling without overt toxicity. In addition, SK-124 causes PTH-like effects at the level of 1,25-vitamin D generation, suggesting that the renal actions of PTH also involve SIK inhibition. Small-molecule SIK inhibitors offer therapeutic advantages over PTH peptide-based therapies such as oral availability, potential to fine-tune pharmacokinetics to optimally stimulate bone formation versus bone resorption, and potential PTH-independent immunomodulatory roles of SIKs downstream of other GPCRs (42, 43). Indeed, SK-124 modulates serum cytokine levels following acute in vivo lipopolysaccharide challenge (*SI Appendix*, Fig. S7) in a manner similar to that of other, less specific SIK inhibitors (20).

It is unlikely that pharmacologic effects of a SIK2/SIK3 inhibitor would ever be as potent as what is observed upon global genetic deletion of these kinases. For example, genetic overexpression of a constitutively active PTH receptor in osteoblasts and osteocytes leads to a dramatic skeletal phenotype similar to that of SIK2/SIK3 gene deletion (44, 45), while pharmacologic intermittent PTH treatment boosts bone mass to a much more modest (yet therapeutically valuable) degree. Future long-term treatment studies are needed to assess the effects of pharmacologic SIK inhibition on cortical bone mass and bone strength.

In light of glucose homeostasis phenotypes seen in global and tissue-specific mice lacking SIK2 (46–48), future studies are needed to understand the consequences of organismal SIK2/SIK3 inhibition. In addition, future studies are needed to determine whether organism-wide SIK2/SIK3 inhibition impacts other physiologic systems where SIKs play an important role such as sleep homeostasis (49), ovarian follicle maturation (50), or melanocyte pigmentation (51). Notably, pharmacologic strategies to deliver small molecules directly to bone may facilitate directed skeletal delivery of selective SIK inhibitors (52). In addition, recent developments in small-molecule "degrader" platforms (so-called proteolysis targeting chimeras (PROTACs)) may facilitate potent and selective SIK2/SIK3 degradation in a tissue-specific manner by linking a derivative of SK-124 to a compound that recruits a bone-specific ubiquitin ligase (53–55).

In sum, these studies identify SK-124 as a useful in vivo tool to probe the biologic actions of SIK2/SIK3 in cells and in vivo. Further studies may be needed to optimize the potency and drug-like features of this compound.

Materials and Methods

Detailed methods are provided in *SI Appendix, Materials and Methods*. Adult-onset ubiquitous deletion of SIK2 and SIK3 was performed in 12-wk-old mice (23), with skeletal phenotypes subsequently assessed by micro-CT and histology. A MARK3-based SIK2 homology model was developed and used for virtual docking followed by in vitro kinase assays and iterative medicinal chemistry. Potent and selective SIK2/SIK3 inhibitors were screened using the Nanosyn kinome platform and in Ocy454 cells. Mice were treated once daily with SK-124 by oral gavage for 3 wk. Serum was collected to measure mineral metabolism parameters. Bone was analyzed using histology, static and dynamic histomorphometry, micro-CT, immunohistochemistry, and RT-qPCR on cortical bone RNA.

Data, Materials, and Software Availability. All study data are included in the article and/or *SI Appendix*.

ACKNOWLEDGMENTS. We thank all members of the Wein Laboratory and MGH Endocrine Unit for thoughtful suggestions. We also thank Robert Lipper, Jan Rosenbaum, Michael Hallen, and Diana Wetmore from the Harrington Discovery Institute for invaluable advice and project support. M.N.W. acknowledges funding support from the NIH (P01DK011794 and R01DK116716), Harrington Discovery Institute, and Radius Health. Micro-CT and bone histomorphometry were performed by the Center for Skeletal Research, an NIH-funded program (P30AR066261, led by Drs. Mary Bouxsein and Marie Demay).

Author affiliations: [a]Endocrine Unit, Massachusetts General Hospital, Harvard Medical School, Boston, MA 02114; [b]Department of Medicine, University of Massachusetts Chan Medical School, Worcester, MA 01655; [c]Horae Gene Therapy Center, University of Massachusetts Chan Medical School, Worcester, MA 01655; [d]Harrington Discovery Institute, University Hospitals, Cleveland, OH 44106; [e]Conifer Point, Doylestown, PA 18902; [f]Radius Health Inc., Boston, MA 02210; [g]Broad Institute of MIT and Harvard, Cambridge, MA 02142; and [h]Harvard Stem Cell Institute, Cambridge, MA 02138

Author contributions: T.S., W.J.G., B.M., B.L., and M.N.W. designed research; T.S., C.D.C.A., S.-H.Y., Y.Z., and D.J.B. performed research; T.S., C.D.C.A., S.-H.Y., Y.Z., W.J.G., P.C.W., U.V., J.K., D.J.B., M.B.D., M.L.B., B.M., B.L., and M.N.W. analyzed data; and T.S., W.J.G., J.K., B.L., and M.N.W. wrote the paper.

1. S. R. Cummings, L. J. Melton, Epidemiology and outcomes of osteoporotic fractures. *Lancet* **359**, 1761–1767 (2002).
2. A. Looker *et al.*, NCHS Data Brief: Osteoporosis or Low Bone Mass at the Femur Neck or Lumbar Spine in Older Adults: United States. *NCHS Centers Dis. Control Prev.* **93**, 2005–2008 (2012).
3. K. E. Ensrud, C. J. Crandall, Bisphosphonates for postmenopausal osteoporosis. *JAMA* **322**, 2017–2018 (2019).
4. P. M. Camacho *et al.*, American Association of clinical endocrinologists and American college of endocrinology clinical practice guidelines for the diagnosis and treatment of postmenopausal osteoporosis-2016. *Endocr. Pract.* **22**, 1–42 (2016).
5. A. Qaseem *et al.*, Treatment of low bone density or osteoporosis to prevent fractures in men and women: A clinical practice guideline update from the American college of physicians. *Ann. Intern. Med.* **166**, 818–839 (2017).
6. B. Z. Leder, Parathyroid hormone and parathyroid hormone-related protein analogs in osteoporosis therapy. *Curr. Osteoporos. Rep.* **15**, 110–119 (2017).
7. I. R. Reid, E. O. Billington, Drug therapy for osteoporosis in older adults. *Lancet* **399**, 1080–1092 (2022).
8. J. Bovijn *et al.*, Evaluating the cardiovascular safety of sclerostin inhibition using evidence from meta-analysis of clinical trials and human genetics. *Sci. Transl. Med.* **12**, eaay6570 (2020).
9. I. Sutkeviciute *et al.*, PTH/PTHrP receptor signaling, allostery, and structures. *Trends. Endocrinol. Metab.* **30**, 860–874 (2019).
10. H. Noda *et al.*, Optimization of PTH/PTHrP hybrid peptides to derive a long-acting PTH analog (LA-PTH). *JBMR Plus* **4**, e10367 (2020).
11. A. D. White *et al.*, Spatial bias in cAMP generation determines biological responses to PTH type 1 receptor activation. *Sci. Signal* **14**, eabc5944 (2021).
12. I. Sutkeviciute *et al.*, Precise druggability of the PTH type 1 receptor. *Nat. Chem. Biol.* **18**, 272–280 (2021).
13. T. Tamura *et al.*, Identification of an orally active small-molecule PTHR1 agonist for the treatment of hypoparathyroidism. *Nat. Commun.* **7**, 13384 (2016).
14. G. Burshtein *et al.*, The combined effect of permeation enhancement and proteolysis inhibition on the systemic exposure of orally administrated peptides: Salcaprozate sodium, soybean trypsin inhibitor, and teriparatide study in pigs. *X* **3**, 100097 (2021).
15. S. Ish-Shalom *et al.*, Safety and efficacy of oral human parathyroid hormone (1–34) in hypoparathyroidism: An open-label study. *J. Bone. Miner. Res.* **36**, 1060–1068 (2021).
16. H. Takemori *et al.*, Salt-inducible kinase-mediated regulation of steroidogenesis at the early stage of ACTH-stimulation. *J. Steroid Biochem. Mol Biol.* **85**, 397–400 (2003).
17. N. J. Darling, P. Cohen, Nuts and bolts of the salt-inducible kinases (SIKs). *Biochem. J.* **478**, 1377–1397 (2021).
18. K. Sakamoto, L. Bultot, O. Goransson, The salt-inducible kinases: Emerging metabolic regulators. *Trends* . **29**, 827–840 (2018).
19. M. N. Wein *et al.*, Salt-inducible kinases: Physiology, regulation by camp, and therapeutic potential. *Trends Endocrinol. Metab.* **29**, 723–735 (2018).
20. T. B. Sundberg *et al.*, Development of chemical probes for investigation of salt-inducible kinase function in vivo. *ACS Chem. Biol.* **11**, 2105–2111 (2016).
21. Y. Tarumoto *et al.*, Salt-inducible kinase inhibition suppresses acute myeloid leukemia progression in vivo. *Blood* **135**, 56–70 (2019).
22. M. N. Wein *et al.*, SIKs control osteocyte responses to parathyroid hormone. *Nat. Commun.* **7**, 13176 (2016).
23. C. C. Tang *et al.*, Dual targeting of salt inducible kinases and CSF1R uncouples bone formation and bone resorption. *Elife* **10**, e67772 (2021).
24. F. Csukasi *et al.*, The PTH/PTHrP-SIK3 pathway affects skeletogenesis through altered mTOR signaling. *Sci. Transl. Med.* **10**, eaat9356 (2018).
25. S. Nishimori *et al.*, Salt-inducible kinases dictate parathyroid hormone 1 receptor action in bone development and remodeling. *J. Clin. Invest.* **129**, 5187–5203 (2019).
26. A. M. Bertorello *et al.*, Increased arterial blood pressure and vascular remodeling in mice lacking salt-inducible kinase 1 (SIK1). *Circ. Res.* **116**, 642–652 (2015).
27. S. Sasagawa *et al.*, SIK3 is essential for chondrocyte hypertrophy during skeletal development in mice. *Development* **139**, 1153–1163 (2012).
28. M. Weise *et al.*, Effects of estrogen on growth plate senescence and epiphyseal fusion. *Proc. Natl. Acad. Sci. U.S.A.* **98**, 6871–6876 (2001).
29. S. Klaeger *et al.*, The target landscape of clinical kinase drugs. *Science* **358**, eaan4368 (2017).
30. S. Lesnik *et al.*, LiSiCA: A software for ligand-based virtual screening and its application for the discovery of butyrylcholinesterase inhibitors. *J. Chem. Inf. Model* **55**, 1521–1528 (2015).
31. L. J. Alvey, Novel compounds and pharmaceutical compositions thereof for the treatment of diseases, Patent number WO2019105886A1 (2019).
32. N. Desroy, Novel compounds and pharmaceutical compositions thereof for the treatment of diseases, Patent number WO2019238424A1 (2019).
33. M. Raab *et al.*, The small-molecule inhibitor MRIA9 reveals novel insights into the cell cycle roles of SIK2 in Ovarian cancer cells. *Cancers* **13**, 3658 (2021).
34. R. Tesch *et al.*, Structure-based design of selective salt-inducible kinase inhibitors. *J. Med. Chem.* **64**, 8142–8160 (2021).
35. J. Bowes *et al.*, Reducing safety-related drug attrition: The use of in vitro pharmacological profiling. *Nat. Rev. Drug Discov.* **11**, 909–922 (2012).
36. M. M. Attwood *et al.*, Trends in kinase drug discovery: Targets, indications and inhibitor design. *Nat. Rev. Drug Discov.* **20**, 839–861 (2021).
37. C. Arter *et al.*, Structural features of the protein kinase domain and targeted binding by small molecule inhibitors. *J. Biol. Chem.* **298**, 102247 (2022).
38. A. F. Rudolf *et al.*, A comparison of protein kinases inhibitor screening methods using both enzymatic activity and binding affinity determination. *PLoS One* **9**, e98800 (2014).
39. H. Y. Jin *et al.*, High-Throughput Implementation of the NanoBRET target engagement intracellular kinase assay to reveal differential compound engagement by SIK2/3 Isoforms. *SLAS Discov.* **25**, 215–222 (2020).
40. D. Martinez Molina *et al.*, Monitoring drug target engagement in cells and tissues using the cellular thermal shift assay. *Science* **341**, 84–87 (2013).
41. R. Baron, M. Kneissel, WNT signaling in bone homeostasis and disease: From human mutations to treatments. *Nat. Med.* **19**, 179–192 (2013).
42. K. Clark *et al.*, Phosphorylation of CRTC3 by the salt-inducible kinases controls the interconversion of classically activated and regulatory macrophages. *Proc. Natl. Acad. Sci. U.S.A.* **109**, 16986–16991 (2012).
43. T. B. Sundberg *et al.*, Small-molecule screening identifies inhibition of salt-inducible kinases as a therapeutic strategy to enhance immunoregulatory functions of dendritic cells. *Proc. Natl. Acad. Sci. U.S.A.* **111**, 12468–12473 (2014).
44. L. M. Calvi *et al.*, Activated parathyroid hormone/parathyroid hormone-related protein receptor in osteoblastic cells differentially affects cortical and trabecular bone. *J. Clin. Invest.* **107**, 277–286 (2001).
45. C. A. O'Brien *et al.*, Control of bone mass and remodeling by PTH receptor signaling in osteocytes. *PLoS One* **3**, e2942 (2008).
46. J. Sakamaki *et al.*, Role of the SIK2-p35-PJA2 complex in pancreatic beta-cell functional compensation. *Nat. Cell Biol.* **16**, 234–244 (2014).
47. J. Park *et al.*, SIK2 is critical in the regulation of lipid homeostasis and adipogenesis in vivo. *Diabetes* **63**, 3659–3673 (2014).
48. K. Patel *et al.*, The LKB1-salt-inducible kinase pathway functions as a key gluconeogenic suppressor in the liver. *Nat. Commun.* **5**, 4535 (2014).
49. H. Funato *et al.*, Forward-genetics analysis of sleep in randomly mutagenized mice. *Nature* **539**, 378–383 (2016).
50. M. Armouti *et al.*, Salt-inducible kinases are critical determinants of female fertility. *Endocrinology* **161**, 069 (2020).
51. N. Mujahid *et al.*, A UV-independent topical small-molecule approach for melanin production in human skin. *Cell Rep.* **19**, 2177–2184 (2017).
52. S. Sun *et al.*, Bisphosphonates for delivering drugs to bone. *Br. J. Pharmacol.* **178**, 2008–2025 (2021).
53. M. Bekes, D. R. Langley, C. M. Crews, PROTAC targeted protein degraders: The past is prologue. *Nat. Rev. Drug Discov.* **21**, 181–200 (2022).
54. K. A. Donovan *et al.*, Mapping the degradable kinome provides a resource for expedited degrader development. *Cell* **183**, 1714–1731.e10 (2020).
55. R. G. Guenette *et al.*, Target and tissue selectivity of PROTAC degraders. *Chem. Soc. Rev.* **51**, 5740–5756 (2022).